REPORT DOCUMENTATION PAGE

Form Approved OMB NO. 0704-0188

1. REPORT DATE (DD-MM-YYYY)	2. REPORT TYPE	3. DATES COVERED (From - To)
	New Reprint	-

4. TITLE AND SUBTITLE
Formation of polarized beams in chains of dielectric spheres and cylinders

5a. CONTRACT NUMBER
W911NF-09-1-0450

5b. GRANT NUMBER

5c. PROGRAM ELEMENT NUMBER
611102

6. AUTHORS
Arash Darafsheh, Neda Mojaverian, Nicholaos I. Limberopoulos, Kenneth W. Allen, Anatole Lupu, Vasily N. Astratov

5d. PROJECT NUMBER

5e. TASK NUMBER

5f. WORK UNIT NUMBER

7. PERFORMING ORGANIZATION NAMES AND ADDRESSES
University of North Carolina - Charlotte
Engineering Technology
9201 University City Boulevard
Charlotte, NC 28223 -0001

8. PERFORMING ORGANIZATION REPORT NUMBER

9. SPONSORING/MONITORING AGENCY NAME(S) AND ADDRESS (ES)
U.S. Army Research Office
P.O. Box 12211
Research Triangle Park, NC 27709-2211

10. SPONSOR/MONITOR'S ACRONYM(S)
ARO

11. SPONSOR/MONITOR'S REPORT NUMBER(S)
54377-MS.31

12. DISTRIBUTION AVAILIBILITY STATEMENT
Approved for public release; distribution is unlimited.

13. SUPPLEMENTARY NOTES
The views, opinions and/or findings contained in this report are those of the author(s) and should not contrued as an official Department of the Army position, policy or decision, unless so designated by other documentation.

14. ABSTRACT
Using numerical modeling, it is shown that chains of dielectric spheres and cylinders act as polarizers. The mechanism is based on gradual filtering of periodically focused modes with a certain polarization propagating with minimal losses due to Brewster angles conditions, whereas orthogonally polarized modes are strongly attenuated. It is shown that chains of cylinders filter linearly polarized beams, whereas chains of spheres filter radially polarized beams. In the geometrical optics limit, we show that in a range of sphere refractive indices 1.68–1.80 a degree of radial polarization in excess of 0.9 can be obtained in 10 sphere long chains.

15. SUBJECT TERMS
Integrating spheres, polarization-sensitive devices, micro-optics, photonic nanojet

16. SECURITY CLASSIFICATION OF:			17. LIMITATION OF ABSTRACT	15. NUMBER OF PAGES	19a. NAME OF RESPONSIBLE PERSON
a. REPORT	b. ABSTRACT	c. THIS PAGE			Vasily Astratov
UU	UU	UU	UU		19b. TELEPHONE NUMBER 704-687-8131

Report Title

Formation of polarized beams in chains of dielectric spheres and cylinders

ABSTRACT

Using numerical modeling, it is shown that chains of dielectric spheres and cylinders act as polarizers. The mechanism is based on gradual filtering of periodically focused modes with a certain polarization propagating with minimal losses due to Brewster angles conditions, whereas orthogonally polarized modes are strongly attenuated. It is shown that chains of cylinders filter linearly polarized beams, whereas chains of spheres filter radially polarized beams. In the geometrical optics limit, we show that in a range of sphere refractive indices 1.68–1.80 a degree of radial polarization in excess of 0.9 can be obtained in 10-sphere-long chains.

REPORT DOCUMENTATION PAGE (SF298)
(Continuation Sheet)

Continuation for Block 13

ARO Report Number 54377.31-MS
Formation of polarized beams in chains of dielec...

Block 13: Supplementary Note

Approved for public release; distribution is unlimited.

Formation of polarized beams in chains of dielectric spheres and cylinders

Arash Darafsheh,[1,4,†] Neda Mojaverian,[2] Nicholaos I. Limberopoulos,[2] Kenneth W. Allen,[1] Anatole Lupu,[3] and Vasily N. Astratov[1,2,5]

[1]*Department of Physics and Optical Science, Center for Optoelectronics and Optical Communications, University of North Carolina at Charlotte, Charlotte, North Carolina 28223-0001, USA*

[2]*Air Force Research Laboratory, Sensors Directorate, Wright Patterson AFB, Ohio 45433, USA*

[3]*Institut d'Electronique Fondamentale, UMR 8622 CNRS, Université Paris-Sud XI, 91405 Orsay, France*

[4]*e-mail: arash.darafsheh@gmail.com*

[5]*e-mail: astratov@uncc.edu*

Received August 5, 2013; revised September 14, 2013; accepted September 17, 2013; posted September 19, 2013 (Doc. ID 195214); published October 14, 2013

Using numerical modeling, it is shown that chains of dielectric spheres and cylinders act as polarizers. The mechanism is based on gradual filtering of periodically focused modes with a certain polarization propagating with minimal losses due to Brewster angles conditions, whereas orthogonally polarized modes are strongly attenuated. It is shown that chains of cylinders filter linearly polarized beams, whereas chains of spheres filter radially polarized beams. In the geometrical optics limit, we show that in a range of sphere refractive indices 1.68–1.80 a degree of radial polarization in excess of 0.9 can be obtained in 10-sphere-long chains. © 2013 Optical Society of America

OCIS codes: (120.3150) Integrating spheres; (130.5440) Polarization-selective devices; (350.3950) Micro-optics.
http://dx.doi.org/10.1364/OL.38.004208

Recently, it was demonstrated that linear arrays of dielectric spheres can operate as lossless waveguides for beams with certain spatial and polarization properties [1]. This can be achieved due to the fact that the Brewster angles conditions are periodically reproduced for modes with a period matching the size of two sphere diameters ($2D$). In the geometrical optics limit, it was shown that such periodically focused modes (PFMs) are radially polarized.

It should be noted that the PFM concept has been stimulated by previous studies of the chains of mesoscale ($D < 10\lambda$, where λ is the wavelength of light) spheres [2] and cylinders [3] performed in the context of coupling between their whispering gallery modes, beam focusing produced by individual spheres and microdisks [4–7] (termed photonic nanojet effect), and coupling between nanojets in chains of spheres [8]. The latter mechanism leads to formation of periodic nanojet-induced modes (NIMs) observed in chains of polystyrene microspheres [9–13] and cylinders [14]. In principle, NIMs in mesoscale spheres can be considered as a wave-optics analog of PFMs introduced [1] in a geometrical optics limit. Some common NIMs and PFMs properties leading to a gradual reduction of the focused beam width [1,9] along the chain and a gradual reduction of the attenuation below 0.1 dB/sphere [1,10] have been reported.

In this work we show that chains of cylinders and spheres can also be used as polarizers with focusing capability. The operation of such structures is based on the fact that their photonic eigenstates are represented by PFMs with orthogonal polarizations, which have dramatically different propagation losses. We first illustrate these effects by finite element method (FEM) simulations for coupled cylinders where the eigenstates are linearly polarized. After that we consider these effects in coupled microspheres where the polarization eigenstates are represented by radially and azimuthally polarized beams. Using ray tracing for sufficiently large spheres ($D \gg 10\lambda$) we show that PFMs with small losses can be obtained in a broad range of refractive indices from $\sqrt{2}$ to 2. We show that high degrees of polarization (DOP), ~0.9, can be obtained in 10-sphere long chains using different ray sources. The polarization filtering and focusing properties display an interesting interplay in chains of spheres so that higher degrees of radial polarization favor sharper focus [15,16] with applications in laser scalpels [17,18], optical tweezers [19], and various focusing devices [20,21].

The results of two-dimensional (2D) FEM modeling of polarization-dependent transmission through a series of dielectric cylinders with refractive index $n = \sqrt{3}$ performed by COMSOL Multiphysics are illustrated in Fig. 1. Launching plane waves polarized along the y axis leads to higher transmission compared to the case of incident waves polarized along the z axis, as can be seen by comparing Figs. 1(a) and 1(b), respectively. In both cases the typical PFM pattern [1] is observed. Higher transmission for incident polarization along the y axis can be explained by the role of the Brewster angle for

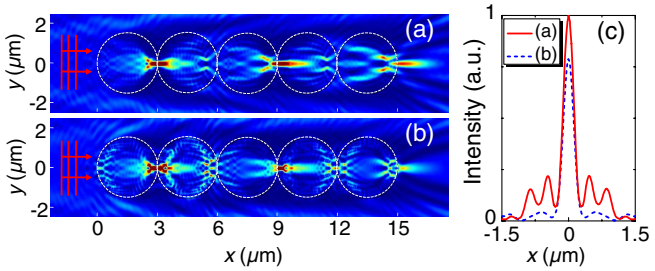

Fig. 1. 2D electric field intensity maps calculated for touching cylinders with $D = 3$ μm and $n = \sqrt{3}$ at $\lambda = 0.53$ μm for the incident plane waves with electric field oscillating along the (a) y axis and (b) z axis. (c) The intensity profiles of the focused beams calculated 0.62 μm away from the tip of the end cylinder showing stronger peak transmission in case (a) compared to (b).

this polarization. Since only a small fraction of the wavefront is incident on the cylinder surface at the Brewster angle, this model cannot be used for quantitative analysis of such mesoscale structures; however it provides a physical explanation of this observation.

Similar ideas can be applied in a more elaborate way to structures formed by macroscopic spheres ($D \gg 10\lambda$) using geometrical optics approximation. Previously, we showed that the exact conditions for Brewster incidence [1] can be satisfied for spheres with refractive index $n = \sqrt{3}$ if collimated TM polarized incident rays are off-axially shifted by $r/D = \sqrt{3}/4$, as illustrated in Fig. 2(a). It is interesting, however, to consider different spheres' indices and study if PFMs can still exist under these conditions. The idea of our analysis is that in order to remain $2D$ periodic, such modes should have different off-axial shifts. Their external (θ_i) and internal (θ_r) angles of incidence and refraction, respectively, would not be exactly equal to those following Brewster's law, but they can be sufficiently close to the optimal values. Most importantly, these angles would be periodically reproduced as light propagates through the chains which would help to keep the losses low.

The collimated incident rays are reproduced with $2D$ period when the refracted ray passes through the point where the spheres touch leading to the following equations: $\theta_i = 2\cos^{-1}(n/2n_b)$, $r/D = 0.5\sin(\theta_i)$, where $n_b = 1$ is the refractive index of the background medium. Based on these equations, it can be deduced that quasi-PFMs exist in a broad range ($\sqrt{2} < n < 2$) of indices. The angle of incidence and axial offset of these modes decrease with the increase in the refractive index.

The attenuation properties of chains of spheres were studied by considering rays forming configurations with $2D$ period. For each index it was achieved by adjusting θ_i and r according to the equations presented above. Propagation losses for the incident rays illustrated in Fig. 2(a) can be estimated by taking into account Fresnel reflection coefficients [22] at each spherical interface from the following equations for TE and TM polarizations:

$$R_{\mathrm{TE}} = \frac{\sin^2(\theta_i/2)}{\sin^2(3\theta_i/2)}, \tag{1}$$

$$R_{\mathrm{TM}} = \frac{\tan^2(\theta_i/2)}{\tan^2(3\theta_i/2)}. \tag{2}$$

The transmittance and corresponding reflection losses for rays with TE and TM polarizations as a function of n for chains of $N = 1, 5, 10$, and 20 spheres are presented in Figs. 2(b) and 2(c), respectively. As expected, regardless of the length of the chain, full transmission and zero reflection loss occurs at $n = \sqrt{3}$ for TM polarization which satisfies the Brewster angles conditions [1]. It is interesting, however, that the high transmission properties are preserved in a broad range of indices around $n = \sqrt{3}$ for TM polarization. It is illustrated in Fig. 2(c) that for 10-sphere long chains with $1.68 < n < 1.80$, TM polarized PFMs have total propagation losses smaller than 1 dB, i.e., less than 0.1 dB/sphere. Conversely, for TE polarization, the total PFM losses exceed 20 dB in the same range of indices. This means that for randomly polarized collimated incident rays, the output mainly has a TM polarization component. Due to axial symmetry of the problem, the global state of polarization of the transmitted beam should be increasingly radial.

To study the polarizing capability of such chains we considered three types of ray sources:

(i) A source of collimated rays with uniform density across the structure and random polarization, as shown in Fig. 3(a). Such rays impinge on the spherical surface at different angles depending on r. Only the TM polarized rays with parameters θ_i and r close to those presented in the above equations can effectively contribute to the transmission through sufficiently long chains. Such source effectively represents a geometrical optics model for illumination with a collimated laser beam.

(ii) A sphere with diameter D that emits rays throughout its volume in all directions with random polarization as shown in Fig. 3(b). This light source (S) can be considered as a model for dye-doped fluorescent

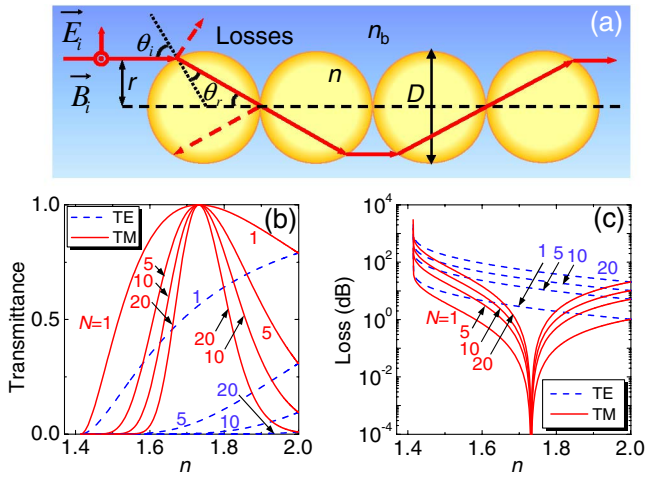

Fig. 2. (a) Ray tracing in an array of identical touching spheres under the condition of periodic propagation. (b) Transmittance and (c) loss in chains of $N = 1, 5, 10$ and 20 spheres as a function of n for TE and TM polarizations of the incident ray. In a geometrical optics limit ($D \gg 10\lambda$) the results are not dependent on D and λ.

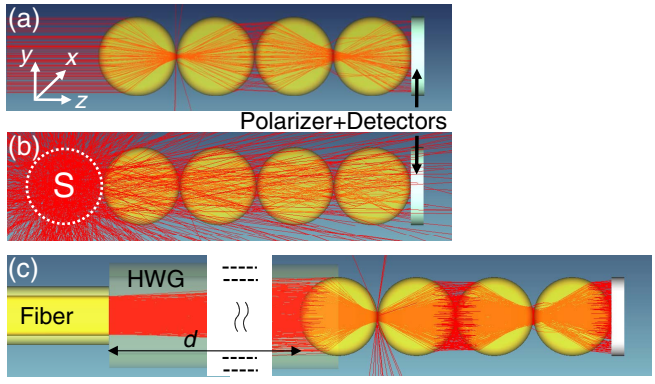

Fig. 3. Three different types of coupling to the PFMs. (a) Collimated rays, (b) spherical emitter, and (c) a multimode fiber inserted inside a hollow waveguide.

microspheres which have been used in experimental studies [1,9–13] of such structures below the lasing threshold for whispering gallery modes. Above this threshold the geometrical optics approximation typically cannot be used and full-wave EM modeling is required [3,23].

(iii) A source of diverging rays mimicking the directionality of multimode fibers with typical divergence angle around 12°. Such directionality can be realized, as an example, in the mid-infrared range using fibers with ~150 μm core diameters, as shown in Fig. 3(c). This type of illumination can take place in focusing devices operating with multimodal beams [17,18]. This light source represents intermediate directional properties between cases (i) and (ii).

The DOP $P(\mathbf{r})$ is defined as the ratio of the (averaged) intensity of the polarized portion of the beam to its total (averaged) intensity, both taken at the same point [24]. This rigorous and unambiguous definition of the DOP is, however, sometimes difficult to use in practical cases. In such situations various *ad hoc* definitions of the DOP are frequently used in the form [24]:

$$Q(\mathbf{r}) = \frac{|I_x(\mathbf{r}) - I_y(\mathbf{r})|}{I_x(\mathbf{r}) + I_y(\mathbf{r})}, \tag{3}$$

where I_x and I_y are the averaged intensities in two mutually orthogonal directions, their choice being suggested by the geometry of the problem. Unlike the $P(\mathbf{r})$, the quantity $Q(\mathbf{r})$ depends on the choice of the x, y axes. It has been theoretically demonstrated, however, that the *ad hoc* definition in the form of Eq. (3) will correctly represent the degree of polarization $P(\mathbf{r})$, provided that I_x and I_y are taken to be true eigenvalues of the polarization matrix representing the symmetry of a given problem [24]. The axial symmetry of the chains of spheres implies that their polarization eigenvalues should be represented by the intensities of radially (I_r) and azimuthally (I_φ) polarized beams.

Typical intensity distribution calculated for spheres with $n = \sqrt{3}$ using a flat detector in contact with the end sphere is illustrated in Fig. 4(a) in the case of collimated incident rays for 20-sphere long chain. This case is representative of the calculations performed for chains formed by even number of spheres with $n = 1.65$–1.85. For this range of indices the output beams consist of a ring with radius r determined by the PFM axial offset, a more compact central beam formed by paraxial rays, and a weak background illumination. The dominant contribution to the output optical power is given by the ring with radius r.

To estimate the DOP, we placed a horizontally oriented linear polarizer (along x) after the end-sphere, as shown in Fig. 4(b). The azimuthal intensity modulation along the ring in Fig. 4(c) carries information about DOP of the transmitted beam. It was studied by using a local detector (extended along x) with dimensions $D/10 \times D/100$ placed after the polarizer, as schematically indicated by a stripe labeled I_r in Figs. 4(b) and 4(c). Such a detector provides a local calculation of the intensity of TM components of transmitted PFMs, which in turn can be taken as a measure of I_r. From the axial symmetry

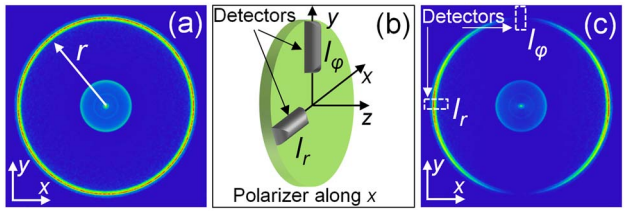

Fig. 4. (a) Intensity distribution produced by a 20-sphere-long chain with $n = \sqrt{3}$ as a result of illumination with collimated rays. (b) Linear polarizer (along x) placed between the end-sphere and the detectors. (c) Intensity distribution with the polarizer installed also showing positions of two detectors (dashed rectangles) used for DOP calculations.

it follows that the measure of the intensity of azimuthally polarized beams can be obtained by using a 90° rotated local detector labeled $I\varphi$ in Figs. 4(b) and 4(c). Using relationships $I_x = I_r$ and $I_y = I_\varphi$ in Eq. (3), we calculated the degree of radial polarization as a function of n for chains with different lengths. We ensured good convergence of the results with reduction of the width of the detectors. Numerical modeling was performed by using ZEMAX-EE.

The results of calculations of DOPs for three types of ray sources are represented in Figs. 5(a)–5(c) in direct correspondence with the structures illustrated in Figs. 3(a)–3(c). It is seen that DOP increases with the length of the chain reaching ~0.9 for 10-sphere chains with $1.68 < n < 1.80$. The highest DOP can be obtained for collimated input beams, as shown in Fig. 5(a). In the case of diverging input beams, illustrated in Fig. 5(c), the DOP values are slightly reduced compared to that in Fig. 5(a).

The DOP calculations for the case of spherical source of rays are illustrated in Fig. 5(b). The spherical source produces a variety of rays with different directionality. A significant fraction of these rays leaks out of the chain in the first few spheres adjacent to S-sphere, as shown in Fig. 3(b). It requires longer propagation distance in this case to establish a typical ring pattern in the transverse intensity distribution similar to that illustrated in Fig. 4(a). Such ring patterns indicate that the PFMs are formed far away from the S-sphere, typically for $N \geq 10$ [1]. In addition, the spherical source is coupled to both fundamental PFMs, one of which is shifted by the sphere diameter D [1]. For this reason, the typical transverse intensity distribution includes the ring representing one fundamental PFM and the central intensity peak

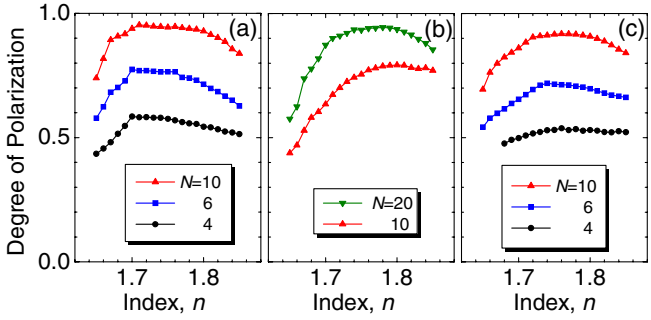

Fig. 5. (a)–(c) Degree of radial polarization versus n calculated for three types of ray sources illustrated in Figs. 3(a)–3(c), respectively.

representing the second fundamental PFM shifted by D. Formation of the ring also makes it possible to apply our technique of DOP determination based on using the polarizer with two stripe-detectors. In the case of a spherical source, the DOP values for a 10-sphere long chain are found to be smaller compared to that for other sources, as seen in Fig. 5(b). However, obtaining DOP in excess of 0.9 is still possible in this case by using longer chains with $N = 20$.

In conclusion, we showed that chains of cylinders and spheres have a common property of low-loss, high-extinction ratio polarization filtering of PFMs with a $2D$ period. Previously, the lossless propagation was demonstrated for rays incident at Brewster angles on spheres with $n = \sqrt{3} \approx 1.73$ [1]. In this work, we showed that this effect should be present for a range of sphere indices $1.68 < n < 1.80$. We showed that the chains of cylinders filter linearly polarized beams, whereas chains of spheres filter radially polarized beams. The optimal refractive index for observation of these effects is very close to the index of one of the best quality infrared materials, sapphire (or ruby) with $n \approx 1.71$ at $\lambda \sim 3\ \mu m$, which means that various practical IR focusing and polarization devices can be built using sapphire cylinders or spheres. In addition, since focusing of radially polarized beams can be sharper than the focusing of unpolarized or linearly polarized beams [15,16], such purely dielectric structures can be very useful in high-resolution polarization imaging and in the design of various devices including focusing microprobes, laser scalpels, and optical tweezers.

This work was supported by the U.S. Army Research Office through Dr. J. T. Prater under Contract No. W911NF-09-1-0450, by the National Science Foundation under grant ECCS-0824067, and by Center for Metamaterials, an NSF I/U CRC, award number 1068050. Also, this work was sponsored by the Air Force Research Laboratory (AFRL/RYD) through the AMMTIAC contract with Alion Science and Technology.

†Arash Darafsheh is currently with the Department of Radiation Oncology, University of Pennsylvania, Philadelphia, Pennsylvania 19104, USA.

References

1. A. Darafsheh and V. N. Astratov, Appl. Phys. Lett. **100**, 061123 (2012).
2. V. N. Astratov, J. P. Franchak, and S. P. Ashili, Appl. Phys. Lett. **85**, 5508 (2004).
3. S. Deng, W. Cai, and V. N. Astratov, Opt. Express **12**, 6468 (2004).
4. Z. Chen, A. Taflove, and V. Backman, Opt. Express **12**, 1214 (2004).
5. P. Ferrand, J. Wenger, A. Devilez, M. Pianta, B. Stout, N. Bonod, E. Popov, and H. Rigneault, Opt. Express **16**, 6930 (2008).
6. A. Heifetz, S. C. Kong, A. V. Sahakian, A. Taflove, and V. Backman, J. Comp. Theor. Nanosci. **6**, 1979 (2009).
7. D. McCloskey, J. J. Wang, and J. F. Donegan, Opt. Express **20**, 128 (2012).
8. Z. Chen, A. Taflove, and V. Backman, Opt. Lett. **31**, 389 (2006).
9. A. M. Kapitonov and V. N. Astratov, Opt. Lett. **32**, 409 (2007).
10. S. Yang and V. N. Astratov, Appl. Phys. Lett. **92**, 261111 (2008).
11. T. Mitsui, Y. Wakayama, T. Onodera, T. Hayashi, N. Ikeda, Y. Sugimoto, T. Takamasu, and H. Oikawa, Adv. Mater. **22**, 3022 (2010).
12. T. Mitsui, T. Onodera, Y. Wakayama, T. Hayashi, N. Ikeda, Y. Sugimoto, T. Takamasu, and H. Oikawa, Opt. Express **19**, 22258 (2011).
13. O. Lecarme, T. P. Rivera, L. Arbez, T. Honeggar, K. Berton, and D. Peyrade, J. Vac. Sci. Technol. B **28**, C6O11 (2010).
14. C.-Y. Liu, Phys. Lett. A **376**, 3261 (2012).
15. R. Dorn, S. Quabis, and G. Leuchs, Phys. Rev. Lett. **91**, 233901 (2003).
16. Q. Zhan, Adv. Opt. Photonics **1**, 1 (2009).
17. A. Darafsheh, A. Fardad, N. M. Fried, A. N. Antoszyk, H. S. Ying, and V. N. Astratov, Opt. Express **19**, 3440 (2011).
18. T. C. Hutchens, A. Darafsheh, A. Fardad, A. N. Antoszyk, H. S. Ying, V. N. Astratov, and N. M. Fried, J. Biomed. Opt. **17**, 068004 (2012).
19. E. Mcleod and C. B. Arnold, Nat. Nanotechnol. **3**, 413 (2008).
20. V. N. Astratov, in *Photonic Microresonator Research and Applications*, I. Chremmos, O. Schwelb, and N. Uzunoglu, eds. (Springer, 2010), pp. 423–457.
21. A. Darafsheh, "Optical super-resolution and periodical focusing effects by dielectric microspheres," Ph.D. dissertation (University of North Carolina at Charlotte, 2013).
22. E. Hecht, *Optics*, 4th ed. (Addison, 2001).
23. A. V. Kanaev, V. N. Astratov, and W. Cai, Appl. Phys. Lett. **88**, 111111 (2006).
24. A. Al-Qasimi, O. Korotkova, D. James, and E. Wolf, Opt. Lett. **32**, 1015 (2007).